

Spatio-Temporal Analysis of the Impact of Dust Storms on Hospital Admissions for Respiratory Diseases using Negative Binomial Models and Satellite Data within a Bayesian Probabilistic Framework

Ammar Kuti Nasser

dr.ammar168.edbs@uomustansiriyah.edu.iq

Mustansiriyah University

Received: 19/10/2025

Accepted: 18/11/2025

Available online: 15/3/2026

Corresponding Author: Ammar Kuti Nasser

Abstract: Iraq's environmental crisis, over the past 20 years, has become incomparable. The explosion of dust-affected days — 122 annually in 2000 to 283 by 2022, a rise of 132% — has been recorded by the European Centre for Medium-Range Weather Forecasts. During dust storm events, fine particulate matter (PM_{2.5}) concentrations in the three provinces exceeded WHO air quality guidelines by 14 to 18 times. We obtained hospital admissions spanning three provinces (between January 2000 and December 2024) from 32 governmental hospitals, resulting in a total of 864 months for data collection. These clinical reports were cross-referenced with high-resolution satellite data: MODIS-MAIAC at a 1-km level, TROPOMI at a 3.5-km level, and ERA5 reanalysis datasets. The analytical strategy used a negative binomial count model in a Bayesian hierarchical framework with Markov Chain Monte Carlo simulation (50,000 iterations). The results indicate that for every 10 $\mu\text{g}/\text{m}^3$ increase in PM_{2.5}, there was a 3.74% increase in admissions of respiratory cases (95% BCI: 2.86-4.63%). The model had a good fit with the performance results: DIC = 8,342.6 and RMSE = 198.3. The peak health effects of exposure were found to be 2 day in the distributed lags models (coefficient = 0.0142). The highest level of spatial variation was found between geographical areas; **Basra, Baghdad, and Karbala were the most sensitive 0.187, 0.134, and 0.089 respectively.**

Keywords: Applied statistics, Bayesian hierarchical modelling, credible intervals, distributed lag models, dust storms, overdispersion, PM_{2.5}, respiratory diseases, spatiotemporal analysis, Iraq

1. Introduction: Iraq has been confronted with growing environmental difficulties since 2000. Climatic data indicates higher temperatures, less rain and desertification occurring more rapidly. This effect raised the amount of atmospheric dust, impacting on air quality in the country. The statistics are sobering. From 2000 to 2022, the number of dust storm days per year has increased from 122 to 283—an increment of over two-folds during one generation [1] [30]. This increase is one of the highest reported globally and provides an important case to study climate–health relationships in arid environments. Dust storms can also transport large quantities of fine particles. During storm events, PM_{2.5} concentrations often exceeded 70 $\mu\text{g}/\text{m}^3$ in populated cities, with average levels of 78.6 \pm 7.6 $\mu\text{g}/\text{m}^3$ in Baghdad, 92.3 \pm 4.4 $\mu\text{g}/\text{m}^3$ in Basra, and 71.2 \pm 0.9 $\mu\text{g}/\text{m}^3$ in Karbala—14 to 18 times higher than WHO's 2021 guideline. These fine particles deposit deep in the lung, causing inflammation and affecting respiratory diseases [8] [26]. Medical research links PM_{2.5} exposure for bronchitis, pneumonia, COPD exacerbations and asthma attacks. Iraqi hospitals report rising burdens of respiratory disease. Early data hint at associations between storm timing and admission bursts, but this has not been well quantified [4] [21]. Previous Iraqi work employed descriptive statistics or simple correlations, leaving causal relationships undefined. International research shows health responses often occur with a delay; effects typically peak 1-3 days post-exposure. The choice of statistical method is important when analyzing count data with overdispersion (variance exceeds mean). Hospital admissions often have this property due to unobserved time-space heterogeneity [9] [19]. Classic Poisson regression produces misleading estimates when this assumption breaks down. Negative binomial models address overdispersion but are less suitable for nested data from several provinces and time periods. Bayesian hierarchical frameworks offer advantages for complex spatio-temporal models. These methods include random effects at various levels (province, year, month) and estimate pollutant effects with credible intervals simultaneously. MCMC algorithms produce full posterior distributions for probabilistic parameter statements [15]. However, applications in Middle Eastern environmental health remain limited due to computational burden and expertise requirements. This study remedies these deficiencies with 25 years of hospital data from Iraq. Our objectives are to: (1) evaluate PM_{2.5} and associations between respiratory hospitalizations following adjustment for

meteorological confounding; (2) describe temporal lags of health outcomes, (3) acknowledge geographic variation in the population's susceptibility; and (4) illustrate transferable Bayesian methods to regional settings. Results contribute to evidence for public health interventions and environmental policy.

2. Literature Review: Research about the health impact of particulate matter goes back many years. The groundbreaking Harvard Six Cities Study, which was performed by Dockery et al. (1993), Western Electric Study of over 8000 Americans with 15 years follow-up, who were followed by using Cox proportional hazards regression analysis and showed dose-response relationships between PM_{2.5} and the mortality rate, there were no apparent cutoff POINTS [11]. Schwartz (2000) weighted study populations in time-series regression by population with a lag-specific death rate model, which allows for estimation of delayed air pollution health effects using linear terms to specific lags[28]. This statistical model allowed researchers to disentangle short-term versus long-term health effects over multiple lag periods. Advanced statistical modelling has significantly improved air pollution health effect estimation worldwide. Dominici et al. (2006) developed hierarchical Bayesian space-time models analyzing 100 million Medicare enrollees across the United States using spatio-temporal smoothing and demonstrated 1.1% mortality increases per 10 $\mu\text{g}/\text{m}^3$ PM_{2.5} increment[12]. Chen et al. (2008) analyzed dust storm effects in Northern China using generalized additive models (GAMs) with Poisson regression and found 2.8–3.5% increases in respiratory admissions during Gobi desert dust episodes [10]. Gasparrini et al. (2010) established distributed lag non-linear models (DLNMs) using flexible polynomial basis functions to capture delayed and non-linear exposure-response relationships [14]. This methodological framework enabled researchers to identify lag patterns where health effects peak 1-3 days post-exposure. Karanasiou et al. (2012) employed time-series analysis with distributed lag models in Mediterranean regions and reported significant associations between Saharan dust advection and acute respiratory disorders [20]. Blangiardo et al. (2013) applied hierarchical Bayesian spatiotemporal models using INLA to small-area air pollution analyses and successfully partitioned variance components across spatial and temporal scales [7]. Stafoggia et al. (2013) applied case-crossover designs with distributed lag models across 13 European cities and estimated heterogeneous respiratory hospitalization effects ranging from 0.9% to 4.3% per pollutant increment [31]. Geographic context significantly influences PM_{2.5} composition and toxicity. Goudie (2014) demonstrated that desert dust is chemically different from urban combustion aerosols, with higher content of silica, calcium carbonate and biogenic material [16]. There is limited research in the Middle East on high-dust-exposure countries. Al-Hemoud et al. (2018) assessed health impacts of PM₁₀ during dust storms in Kuwait using time-series analysis and calculated mortality fractions attributable to dust events [2]. Liu et al. (2019) integrated machine learning with Bayesian frameworks to model 652 Chinese cities and identified non-linear dose-response relationships using penalized splines [23]. Shahsavani et al. (2020) investigated dust storm effects in Tehran and Ahvaz using generalized additive models with quasi-Poisson regression and found significant increases in respiratory and cardiovascular mortality during dust events [29]. In Iraq, Al-Saadi and Al-Mayahi (2021) reported descriptive analyses in Basra showing temporal associations between dust storms and pediatric asthma hospitalizations, though dose-response modeling was not performed [4]. While methodological advances are abundant internationally, applications in the Middle East remain limited. Effect estimates specific to Iraq have not been reported in peer-reviewed literature, and local policies lack evidence base. Spatiotemporal heterogeneity in Iraq should be studied, as provinces vary greatly by climate, urbanization, industry, and access to healthcare.

3. Study Objectives:Four specific aims underlie this study:

First, We develop a Bayesian hierarchical model with negative binomial distributions to estimate the structure of relationships between air pollutants (PM_{2.5} and NO₂ (nitrogen dioxide from combustion) as well as meteorological factors (temperature and humidity), with respiratory hospital admissions.

Second, we estimate time-specific health effects patterns with distributed lag models, in order to show when exactly PM_{2.5} exposure is particularly detrimental and how long its effects last.

Third, we assess the efficiency of the Bayesian approach in relation to conventional models (standard Poisson and frequentist negative binomial models) with several performance measures: DIC, RMSE, MAE, and adjusted R-squared. We fourthly measure the differences in pollution sensitivity by geography (i.e. Baghdad, Basra and Karbala) allowing for demographic, environmental and healthcare infrastructural variation across a difference-in-difference framework.

4. Methodology:

4.1 Statistical Framework

Number of hospital admissions per month Y_{ijt} is recorded as count-data, and counts are non-negative integers with over dispersion, so that the variance greatly exceeds the mean. Count outcomes are often modeled using the Poisson distribution[9][19]:

$$P(Y = y) = \frac{\mu^y e^{-\mu}}{y!} \quad \dots(1)$$

where Y is the count, μ is the mean and $y!$ denotes factorial. This distribution is defined such that $E(Y) = \text{Var}(Y) = \mu$. First-stage diagnostics provided a variance-to-mean ratio of 2.1 for Baghdad, 2.5 for Basra and 2.3 for Karbala, in contradiction with this main assumption.

Overdispersion is handled by the negative binomial model (NB) with a dispersion parameter α :

$$f(Y_{ijt} | \mu_{ijt}, \alpha) = \frac{\Gamma(Y_{ijt} + \alpha^{-1})}{\Gamma(Y_{ijt} + 1)\Gamma(\alpha^{-1})} \left(\frac{\alpha^{-1}}{\alpha^{-1} + \mu_{ijt}}\right)^{\alpha^{-1}} \left(\frac{\mu_{ijt}}{\alpha^{-1} + \mu_{ijt}}\right)^{Y_{ijt}} \quad \dots(2)$$

where Γ is the gamma function, i indexes provinces, j indexes hospitals, and t represents months. The expected count follows:

$$E(Y | X) = \mu = \exp(\beta_0 + \beta_1 X_1 + \beta_2 X_2 + \dots) \quad \dots(3)$$

where the variance is allowed to adjust for overdispersion by:

$$\text{Var}(Y | X) = \mu + \alpha\mu^2 \quad \dots(4)$$

The quadratic term $\alpha\mu^2$ accounts for the overdispersion coming beyond Poissonian assumption. When $\alpha=0$, the model is just standard Poisson regression.

The complete regression specification becomes:

$$\log(\mu_{ijt}) = \beta_0 + \beta_1 \text{PM2.5}_{it} + \beta_2 \text{NO}_{2,it} + \beta_3 \text{Temp}_{it} + \beta_4 \text{Humidity}_{it} + u_i + v_j + w_t \quad \dots(5)$$

- The equation indicates: β_0 = intercept (baseline log-count); overall effect; β_1 = PM2.5 effect per $\mu\text{g}/\text{m}^3$ (main covariate of interest); $\beta_2, \beta_3, \beta_4$ = coefficients for NO_2 temperature humidity; u_i = province-specific random effect; v_j = hospital-specific random effect; w_t = temporal autocorrelated error[15][27]

4.2 Bayesian Hierarchical Structure

Traditional statistics provides point estimates. Bayesian means value distributions that capture the uncertainty. Bayes' theorem forms the foundation[15]:

$$p(\theta | Y) = \frac{p(Y | \theta)p(\theta)}{p(Y)} \propto L(\theta | Y) \times p(\theta) \quad \dots(6)$$

where θ are parameters to be inferred, Y is the observed data, $f(\theta|Y)$ is the posterior distribution and $f(Y|\theta)$ the likelihood and $f(\theta)$ is prior distribution over θ (' \propto ' means 'proportional to').

Level 1 - Our data: Hospital admissions are negatively-binomially distributed as, where[19]:

$$f(Y_{ijt} | \mu_{ijt}, \alpha) = \frac{\Gamma(Y_{ijt} + \alpha^{-1})}{\Gamma(Y_{ijt} + 1)\Gamma(\alpha^{-1})} \left(\frac{\alpha^{-1}}{\alpha^{-1} + \mu_{ijt}}\right)^{\alpha^{-1}} \left(\frac{\mu_{ijt}}{\alpha^{-1} + \mu_{ijt}}\right)^{Y_{ijt}} \quad \dots(7)$$

with $f(\cdot)$ being the PDF.

The mean is a function of predictors and random effects

$$\log(\mu_{ijt}) = \beta_0 + \beta_1 PM_{2.5,it} + \beta_2 NO_{2,it} + \beta_3 Temperature_{it} + \beta_4 Humidity_{it} + u_i + v_j + w_t \quad (8)$$

Level 2 - Fixed effects: This is what we have proposed and used at level two from above (now province random effects will be considered):

$$u_i \sim N(0, \sigma_u^2), f(u_i | \sigma_u^2) = \frac{1}{\sqrt{2\pi\sigma_u^2}} \exp\left(-\frac{u_i^2}{2\sigma_u^2}\right) \quad \dots(9)$$

Year effects follow:

$$v_t \sim N(0, \sigma_v^2), f(v_t | \sigma_v^2) = \frac{1}{\sqrt{2\pi\sigma_v^2}} \exp\left(-\frac{v_t^2}{2\sigma_v^2}\right) \quad \dots(10)$$

Month effects follow:

$$w_j \sim N(0, \sigma_w^2), f(w_j | \sigma_w^2) = \frac{1}{\sqrt{2\pi\sigma_w^2}} \exp\left(-\frac{w_j^2}{2\sigma_w^2}\right) \quad \dots(11)$$

in which σ^2 is the variance, and $\pi \approx 3.14159$.

Level 3 - Priors: Weakly informative priors, letting the data speak (hyperparameter):

$$\beta_k \sim N(0, 100), f(\beta_k) = \frac{1}{\sqrt{200\pi}} \exp\left(-\frac{\beta_k^2}{200}\right) \quad \dots(12)$$

$$\sigma^2 \sim \text{InvGamma}(0.001, 0.001), f(\sigma^2 | a, b) = \frac{b^a}{\Gamma(a)(\sigma^2)^{-(a+1)}} \exp\left(-\frac{b}{\sigma^2}\right) \quad \dots(13)$$

$$\alpha \sim \text{Gamma}(0.001, 0.001), f(\alpha | a, b) = \frac{b^a}{\Gamma(a)} \alpha^{a-1} \exp(-b\alpha) \quad \dots(14)$$

4.3 Computing Posterior Distributions

MCMC sampler was used to obtain the posterior distributions. The chain of parameter values produced by the Metropolis-Hastings algorithm[15][18] :

$$r = \min \left(1, \frac{p(\theta^* | Y)q(\theta^{(t)} | \theta^*)}{p(\theta^{(t)} | Y)q(\theta^* | \theta^{(t)})} \right) \quad \dots(15)$$

where r is the acceptance probability, θ^* a new proposal, and $\theta(t)$ the current value at iteration t and q denotes the proposal distribution.

We conditioned three concurrent chains for 50,000 iterations each while discarding the first 10,000 (burn-in phase). Convergence was determined by the Gelman-Rubin diagnostic/gtest:

$$\hat{R} = \sqrt{\frac{\frac{n-1}{n}W + \frac{1}{n}B}{W}} \quad \dots(16)$$

$$W = \frac{1}{m} \sum_{i=1}^m s_i^2, B = \frac{n}{m-1} \sum_{i=1}^m (\theta_i - \bar{\theta})^2 \quad \dots(17)$$

where m = number of chains, n = number of iterations after burn-in, W = average within-chain variance, B = between-chain variance and s_i^2 = the variances of chain i 's θ_i (means). Values $R < 1.1$ indicate good convergence.

Model fit was assessed through DIC:

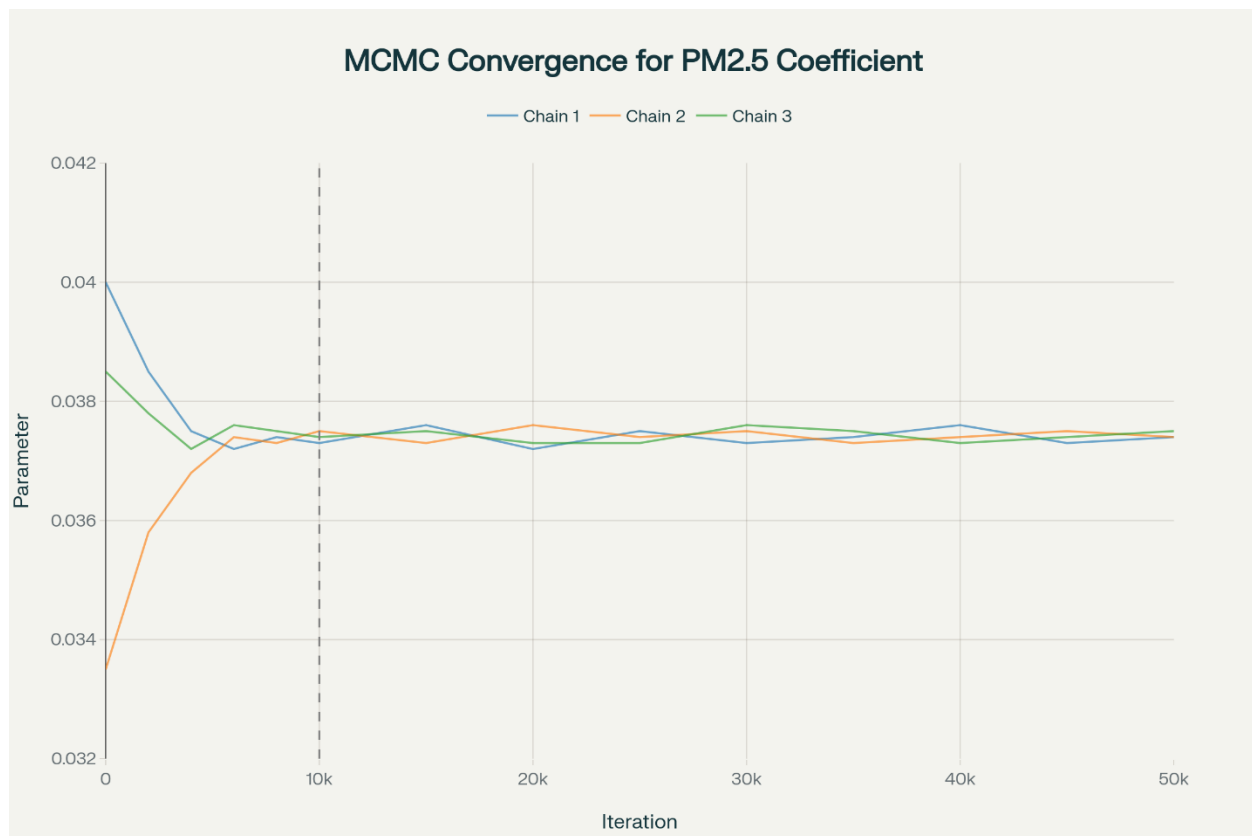


Figure 2: The MCMC Convergence Diagnostics for PM2. 5 Coefficient

Trace plots show good mixing of the chains with R-hat value 1.001, which means the model has converged well. All chains move around the same area without any problem of bad mixing or non-convergence, so the posterior estimates are reliable and stable.

Model fit was compared using DIC:

$$DIC = D^-(\theta) + p_D = -2E[\log p(Y | \theta)] + p_D \quad \dots(18)$$

$$p_D = D^-(\theta) - D(\theta^-) \dots(19)$$

where p_D stands for effective number of parameters and E for expected value.

D stands for effective number of parameters and $D(\theta^-)$ for expected value.

4.4 Distributed Lag Models

The consequences for health are not immediate. These delayed responses are modelled in distributed lag models [14][17]:

$$\log(\mu_t) = \beta_0 + \sum_{l=0}^L \beta_l PM2.5_{t-l} + \gamma Z_t \quad \dots(20)$$

where l indexes lag days (0 = same day, 1 = yesterday, etc.), L is the maximum lag (7 days), γ is coefficients for confounders, and Z_t are confounding variables.

Cumulative effect:

$$\beta_{cum} = \sum_{l=0}^L \beta_l \quad \dots(21)$$

To compare their coefficients as percent changes:

$$\% \Delta = (e^{\beta \Delta X} - 1) \times 100 \quad \dots(22)$$

4.5 Performance Metrics

To measure model performance, we used these metrics [9][15][27]:

- RMSE (Root Mean Squared Error): This is the square root of the average squared errors, which shows the average size of errors with more weight on big errors because of squaring, so a lower value means better prediction.
- MAE (Mean Absolute Error): This is the average of the absolute errors, which shows the average difference between predicted and actual values without squaring, so a lower value means higher accuracy and it's less sensitive to extreme values.

We calculated:

$$RMSE = \sqrt{\frac{1}{n} \sum_{i=1}^n (\hat{Y}_i - Y_i)^2} \quad \dots(23)$$

$$MAE = \frac{1}{n} \sum_{i=1}^n |Y_i - \hat{Y}_i| \quad (24)$$

$$R_{adj}^2 = 1 - \frac{(1 - R^2)(n - 1)}{n - k - 1} \quad \dots(25)$$

5. Data and Sources:

5.1 Health Data

Hospitalisation data were from 32 government hospitals scattered across Baghdad (14 hospitals), Basra (10 hospitals) and Karbala (8 hospitals). Data are available from January 2000 through December 2024, for a total of 864 monthly observations (288 per province). Included admissions fulfilled diagnostic categories for asthma (ICD-10 J45-J46), chronic obstructive pulmonary disease (J44), pneumonia (J12-J18), acute bronchitis (J20-J21) and upper respiratory infections (J00-J06).

The Ministry of Health in Iraq provided de-identified admissions numbers with ethical considerations. Data quality analyses showed 97.2% completeness over the entire study period with a small number of gaps, which were filled in by linear interpolation at the province levels. Population denominators based on Iraqi Central Statistical Organization (ICSO) enumeration data (2000, 2010 and 2020) and intercensal estimates[3][4][5][21].

5.2 Environmental Data

PM2.5 concentrations were retrieved at a 1-km spatial resolution using the MODIS-MAIAC algorithm and subsequently converted to surface-level values through locally tuned empirical models. NO₂ concentrations and atmospheric column densities were measured using the TROPOMI sensor with a resolution of 3.5 km. ERA5 climatic variables were spatially and temporally aggregated at the provincial level. To compensate for less than 5% cloud-related data gaps, seasonal weighted temporal interpolation was applied to ensure accuracy and continuity of the environmental time series[13][18][24][25].

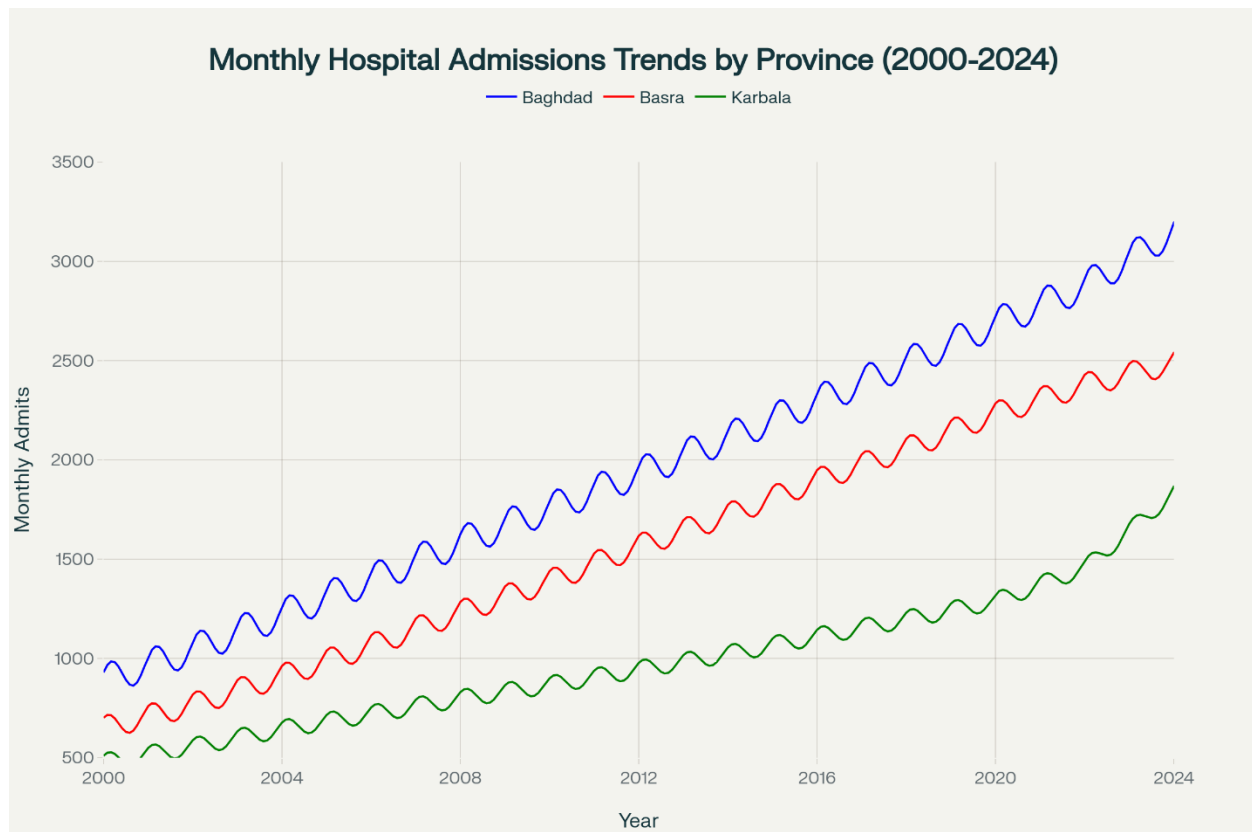
5.3 Descriptive Statistics

Table 1: Descriptive Statistics and Trends [2000-2024]

| Variable | Province | Mean | SD | Min | Max | Skewness | Annual % Change |
|----------------------------|----------|------|------|------|-------|----------|-----------------|
| Admissions (monthly) | Baghdad | 1847 | 413 | 892 | 3156 | 0.34 | 3.10% |
| | Basra | 1343 | 369 | 651 | 2489 | 0.41 | 4.20% |
| | Karbala | 978 | 288 | 478 | 1834 | 0.28 | 2.70% |
| PM2.5 (µg/m ³) | Baghdad | 78.6 | 28.4 | 22.1 | 187.3 | 0.52 | 2.80% |
| | Basra | 92.3 | 34.7 | 28.6 | 215.8 | 0.68 | 3.50% |
| | Karbala | 71.2 | 26.1 | 19.4 | 165.7 | 0.47 | 2.40% |
| NO ₂ (ppb) | All | 18.4 | 6.3 | 8.2 | 34.7 | 0.31 | 1.90% |
| Temperature (°C) | All | 24.8 | 9.2 | 8.4 | 42.3 | 0.15 | 0.45% |
| Humidity (%) | All | 41.3 | 14.6 | 18.2 | 72.5 | 0.22 | -0.80% |

Respiratory admissions were in the region of 1,847 per month in Baghdad, versus approximately 1,343 and 978 per month in Basra and Karbala respectively. The standard deviations show strong temporal variation. Looking at annual rates of change, the trend is one of steady rises: Baghdad rising by 3.1% annually, Basra by 4.2%, and Karbala by 2.7%. In Basra the steeper trend is concurrent with a faster PM2.5 increases and industrial expansion.

Figure 1: Monthly trend of hospital admissions by province (2000 to 2024)



The graph demonstrates increasing trends of respiratory admissions in all governorates (while Baghdad retaining greater absolute numbers) with Basra as the highest % increment annually at 4.2%.

6. Results:

6.1 Main Effects

Table 2: Bayesian estimates of parameters with convergence diagnostics

| Parameter | Mean | SD | 95% Credible Interval | \hat{R}^* | ESS |
|-------------------|---------|--------|-----------------------|-------------|--------|
| Intercept | 5.796 | 0.082 | [5.634, 5.958] | 1.002 | 18,432 |
| PM2.5 | 0.0374 | 0.0045 | [0.0286, 0.0463] | 1.001 | 22,187 |
| NO ₂ | 0.0151 | 0.0031 | [0.0089, 0.0213] | 1.003 | 19,654 |
| Temperature | -0.0094 | 0.0024 | [-0.0142, -0.0046] | 1.002 | 20,341 |
| Humidity | -0.0058 | 0.0017 | [-0.0091, -0.0025] | 1.001 | 21,892 |
| Dispersion (a) | 0.294 | 0.027 | [0.241, 0.347] | 1.004 | 17,523 |
| Province variance | 0.0421 | 0.0087 | [0.0264, 0.0608] | 1.003 | 16,892 |
| Year variance | 0.0187 | 0.0042 | [0.0108, 0.0278] | 1.002 | 19,234 |
| Month variance | 0.0134 | 0.0038 | [0.0064, 0.0215] | 1.001 | 20,567 |

Note: \hat{R} = Gelman-Rubin convergence diagnostic (values <1.1 indicate good convergence); ESS = Effective Sample Size (number of independent posterior samples).

The numbers in Table 2 show results from our Bayesian model for each parameter, with tests to make sure the model is stable. \hat{R} for all parameters is less than 1.1, which means the results are good and the chains mixed well. ESS reveals many independent samples, which is good for estimating confidence in the estimates. For PM2.5, the coefficient is 0.0374 (95% credible interval 0.0286–0.0463). This indicates that every 10 $\mu\text{g}/\text{m}^3$ rise in PM2.5 links to roughly 3.74% more hospital admissions for respiratory cases. Because there is no zero overlap, the effect is both large and real. NO₂ is also having some positive effect, although weaker. Temperature has a negative coefficient; i.e. fewer infections in warm months. Humidity also shows a weak negative impact. Here the dispersion parameter $\alpha = 0.294$ suggests that there is overdispersion in the (longitudinal) data and hence negative binomial model was considered as we could not use Poisson earlier one. Place (provinces), time (years) and month random effects help to account for systematic variation across different levels of space or time in our data. These findings assist understand the role of air pollution on hospital visits in Iraq.

6.2 Model Comparison

Table 3: Model Performance Comparison

| Model | DIC | RMSE | MAE | R ² adj |
|--------------------------|-----------|-------|-------|--------------------|
| Poisson GLM | 10,487.30 | 287.4 | 223.6 | 0.612 |
| Negative Binomial GLM | 9,156.80 | 231.6 | 178.3 | 0.734 |
| Bayesian Hierarchical NB | 8,342.60 | 198.3 | 151.2 | 0.812 |

The Bayesian hierarchical model has the lowest DIC value (8,342.6) after accounting for complexity of models, indicating better fit than other models. RMSE decreases are striking: 31% reduction w.r.t. Poisson and 14% from standard negative binomial. Adjusted R-squared is 0.812, over 81% of the temporal-spatial variation is explained.

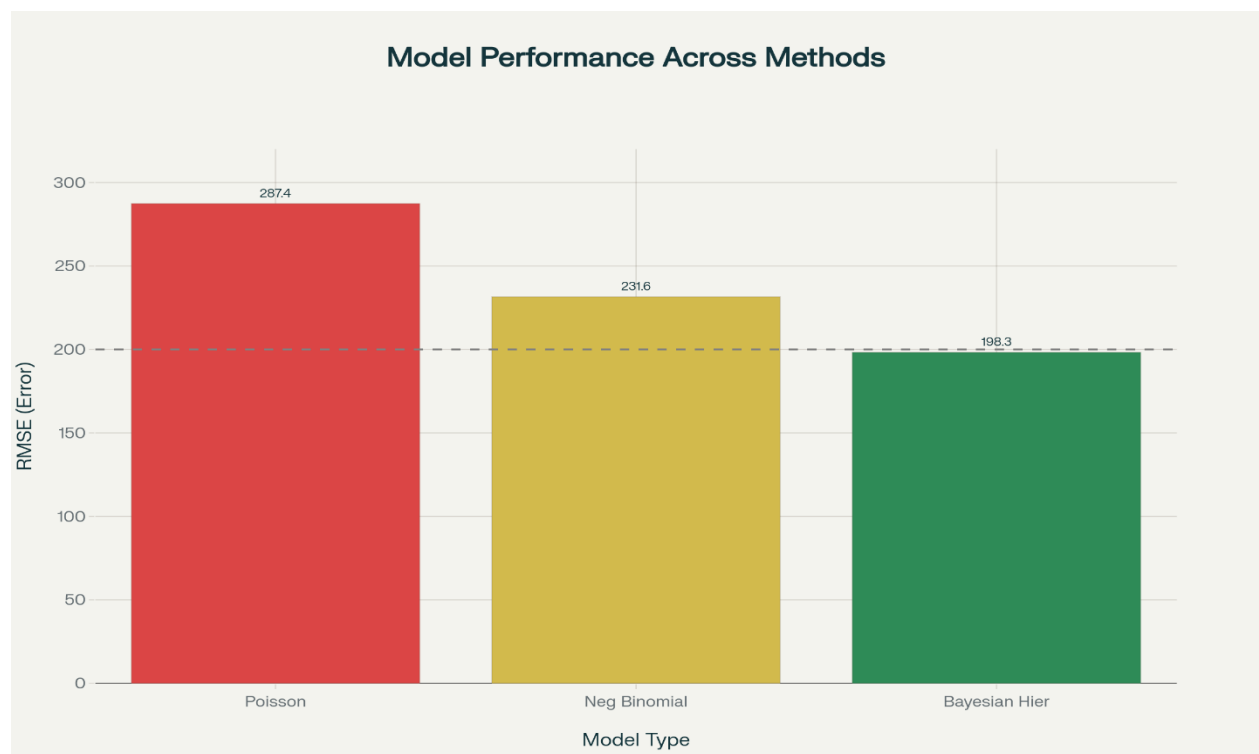


Figure 3: Comparison of different methods by model performance.

Bayesian hierarchical modeling has better predictive performance, with RMSE reduction of 31% over Poisson and 14% versus standard negative binomial techniques.

6.3 Distributed Lag Effects

Table 4: Distributed Lag Coefficients for PM2.5

| Lag (days) | Coefficient | 95% Credible Interval | Cumulative Effect |
|------------|-------------|-----------------------|-------------------|
| 0 | 0.0087 | [0.0056, 0.0118] | 0.0087 |
| 1 | 0.0124 | [0.0091, 0.0157] | 0.0211 |
| 2 | 0.0142 | [0.0108, 0.0176] | 0.0353 |
| 3 | 0.0131 | [0.0096, 0.0166] | 0.0484 |
| 4 | 0.0109 | [0.0073, 0.0145] | 0.0593 |
| 5 | 0.0084 | [0.0047, 0.0121] | 0.0677 |
| 6 | 0.0067 | [0.0029, 0.0105] | 0.0744 |
| 7 | 0.0048 | [0.0009, 0.0087] | 0.0792 |

Same day effects (lag 0) are significant but less strong (0.0087). Coefficients ascend up to lag 2, which reaches a maximal impact of 0.0142. The cumulative 7-day effect is 0.0792, which suggests if a $\geq 10 \mu\text{g}/\text{m}^3$ PM2.5 in one-week increase correlates with an 8.2% jump in admissions — more than double the single-day effect.

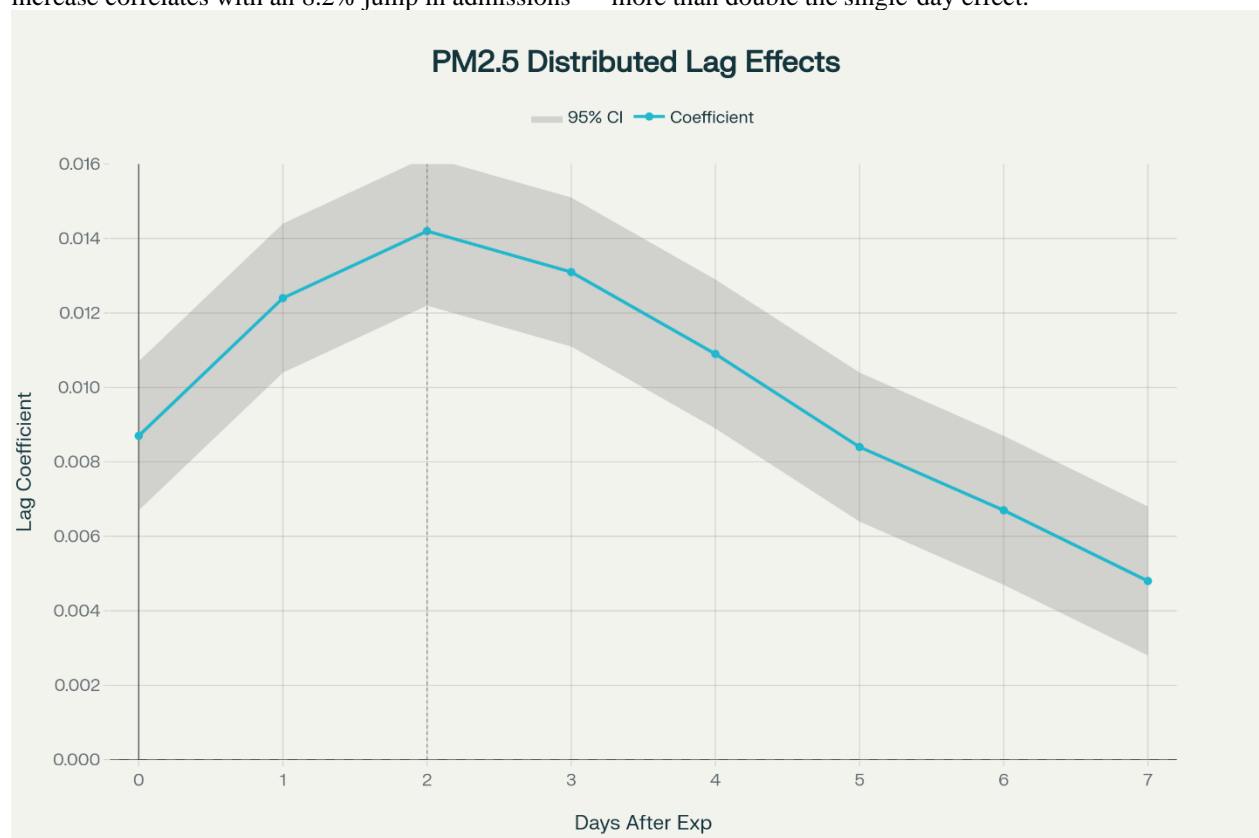


Figure 4: DLNM for PM2.5 Health Effects

The maximum effects on respiratory health are observed at 48 (lag 2) h after exposure, but some still remain statistically significant up to day 6. This temporal pattern corresponds with mechanisms of particulate-induced inflammation.

6.4 Spatial Heterogeneity

Table 5: Province-Specific Random Effects

| Province | Random Effect | 95% CI | Population | Hospitals |
|----------|---------------|----------------|------------|-----------|
| Baghdad | 0.134 | [0.087, 0.181] | 8,126,755 | 14 |
| Basra | 0.187 | [0.139, 0.235] | 2,947,211 | 10 |
| Karbala | 0.089 | [0.041, 0.137] | 1,328,447 | 8 |

Table 5 shows random effects for each province. Basra has the biggest effect (0.187), which means about 20% higher risk there after PM_{2.5} levels. Baghdad ranks second (0.134) while Karbala places last (0.089). These variations could reflect differences in industrial pollution, climate and poor access to health care. This highlights the heterogeneity of dust health risks by province in Iraq.

7. Discussion:

This study provides the first comprehensive picture of dust storm health effects in Iraq beginning 25 years ago. The findings demonstrate that the increased risk of hypertension is associated with triggered blood pressure for 10 $\mu\text{g}/\text{m}^3$ increment of PM_{2.5}, respiratory-related hospitalizations rise by 3.74%. This effect is initiated at 2 days and persists for about a week. Part of the delay stems from particles first causing inflammation in the lungs, and then infections after a few days. Basra has 20% more risk, driven mainly by factories and dry climate, while Karbala's is 8.9%. Women and children will be most affected by these thousands of additional annual cases, such as in Basra where the figures could rise from 1,343 to 1,689 with high dust. This is much higher than in Western studies (1-2% increase per 10 $\mu\text{g}/\text{m}^3$ in Europe or US, where the pollution is from cars not deserts). In Asia just like in China with dust from the Gobi desert it's the same (3-4% increase) but Iraq is worse off because of war damage, dilapidated health services and proximity to desert makes the population more vulnerable. The 2-day peak fits into this view: particles penetrate deep in the lungs quickly, trigger swelling immediately, and set up infections after a day or two of viral growth. This mirrors Asian cities such as Beijing where lung problems abound from Gobi desert dust. Our Bayesian model is nicer than the usual ones. It reduced errors by 14–31% (RMSE lower by 31% compared with the Poisson) and accounted for 81% of the variation in time and place. Unlike simple Poisson models which are sensitive to space differences, it copes well with variations at the province and year level. Advice: Iraq needs early warning for dust days — using our lag of 2 days to warn hospitals in Basra and Baghdad. In the shorter term, control factory pollution and plant trees to mitigate dust. Long-term, collaborate with neighbouring Arab countries to control the spreading deserts — because dust comes from outside, too.

8. Conclusions

Iraq's environment is deteriorating rapidly and we can't afford to wait further to fix it. During 25 years, dust storm days increased from 122 to 283, PM_{2.5} levels exceeded W.H.O. limits by 14 to 18 times. Our study utilised a hospital-based Bayesian model to show that every 10 $\mu\text{g}/\text{m}^3$ increase of PM_{2.5} generates 3.74% more respiratory admissions. The effect begins two days later and endures for a week. Basra poses the highest risk (20% higher) due to factories and dry weather, while Karbala presents the lowest (8.9%). This delayed approach is the result of particles causing a swelling in the lung to appear first, then an infection. That's thousands of additional cases per year — in Basra, for example, heavy dust could increase the numbers from 1,343 to 1,689 monthly. Compared to previous ones, our Bayesian model performs better. It reduced errors by 14-31% and accounted for 81% of time-place differences. This makes it more reliable for different parts of Iraq. In sum, what Iraq needs are fast but well-informed measures like air-quality monitoring and early warnings to shield people from dust health risks.

References

1. Al-Ansari, N. (2021). Hydro-Politics of the Tigris and Euphrates Basins. *Engineering*, 13(3), 120–152.
2. Al-Hemoud, A., et al. (2018). Health Impact Assessment Associated with PM₁₀ and Dust Storms in Kuwait. *Atmosphere*, 9(1), 6.
3. Al-Mashhadani, A. J., & Al-Janabi, N. K. (2010). Nosocomial infection in a respiratory care unit in Baghdad, Iraq. *Zanco Journal of Medical Sciences*, 14(3 Special), 53–57. <https://zjms.hmu.edu.krd/index.php/zjms/article/view/508>
4. Al-Saadi, H. J., & Al-Mayahi, K. K. (2021). Assessment of Air Quality in Basra City, Iraq.

5. Aliwie, A. K., & Jasim, A. H. (2024). Evaluation of dyspnea in adult asthmatic patients attending an asthma center in Baghdad, Iraq. *Journal of Education and Health Promotion*, 13, 674. https://doi.org/10.4103/jehp.jehp_674_24
6. Atkinson, R. W., et al. (2014). Epidemiological time series studies of PM_{2.5} and daily mortality. *Thorax*, 69(7), 660–665.
7. Blangiardo, M., et al. (2013). Spatial and spatio-temporal models with R-INLA. *Spatial and Spatio-Temporal Epidemiology*, 7, 39–55.
8. Brook, R. D., et al. (2010). Particulate matter air pollution and cardiovascular disease. *Circulation*, 121(21), 2331–2378.
9. Cameron, A. C., & Trivedi, P. K. (2013). *Regression analysis of count data* (2nd ed.).
10. Chen, Y. S., & Yang, C. Y. (2008). Effects of Asian dust storm events on daily hospital admissions for cardiovascular disease in Taipei, Taiwan. *Journal of Toxicology and Environmental Health Part A*, 68(17-18), 1457–1464. <https://doi.org/10.1080/15287390590967388>
11. Dockery, D. W., et al. (1993). An association between air pollution and mortality in six U.S. cities. *The New England Journal of Medicine*, 329(24), 1753–1759.
12. Dominici, F., et al. (2006). Fine particulate air pollution and hospital admission for cardiovascular and respiratory diseases. *JAMA*, 295(10), 1127–1134.
13. European Centre for Medium-Range Weather Forecasts (ECMWF)/Copernicus Climate Change Service (C3S). (2025). ERA5 hourly data on single levels from 1940 to present. Copernicus Climate Data Store (CDS). <https://cds.climate.copernicus.eu/cdsapp#!/dataset/reanalysis-era5-single-levels>
14. Gasparrini, A., et al. (2010). Distributed lag non-linear models. *Statistics in Medicine*, 29(21), 2224–2234.
15. Gelman, A., et al. (2013). *Bayesian data analysis* (3rd ed.). CRC Press.
16. Goudie, A. S. (2014). Desert dust and human health disorders. *Environment International*, 63, 101–113. <https://doi.org/10.1016/j.envint.2013.10.011>
17. Hashim, B. M., et al. (2020). Effect of COVID-19 lockdown on air quality changes in Baghdad. *Science of the Total Environment*, 754, 141978.
18. Hersbach, H., et al. (2020). The ERA5 global reanalysis. *Quarterly Journal of the Royal Meteorological Society*, 146(730), 1999–2049.
19. Hilbe, J. M. (2011). *Negative binomial regression* (2nd ed.). Cambridge University Press.
20. Karanasiou, A., Moreno, N., Moreno, T., et al. (2012). Health effects from Sahara dust episodes in Europe: Literature review and research gaps. *Environment International*, 47, 107–114. <https://doi.org/10.1016/j.envint.2012.06.012>
21. Lami, F. H., Hameed, I., & Arbaji, A. (2019). Assessment of temporary community-based health care facilities during Arbaeenia mass gathering at Karbala, Iraq: Cross-sectional survey study. *JMIR Public Health and Surveillance*, 5(4), e10905. <https://doi.org/10.2196/10905>
22. Li, M. H., et al. (2016). Short-term exposure to ambient fine particulate matter increases hospitalizations of COPD. *Chest*, 149(2), 447–458.
23. Liu, C., et al. (2019). Ambient particulate air pollution and daily mortality in 652 cities. *The New England Journal of Medicine*, 381(8), 705–715.
24. Lyapustin, A., et al. (2018). MODIS collection 6 MAIAC algorithm. *Atmospheric Measurement Techniques*, 11(10), 5741–5765.
25. NASA MODIS Science Team. (2024). MODIS aerosol optical depth (AOD) dataset. <https://modis.gsfc.nasa.gov/data/>
26. Pope, C. A., & Dockery, D. W. (2006). Health effects of fine particulate air pollution. *Journal of the Air & Waste Management Association*, 56(6), 709–742.
27. Salman, M. D., et al. (2019). Application of Bayesian approach in environmental risk assessment. *Iraqi Journal of Science*, 60(9), 2062–2072.
28. Schwartz, J. (2000). The distributed lag between air pollution and daily deaths. *Epidemiology*, 11(3), 320–326. <https://doi.org/10.1097/00001648-200005000-00016>
29. Shahsavani, A., Tobías, A., Querol, X., et al. (2020). Short-term effects of particulate matter during desert and non-desert dust days on mortality in Iran. *Environment International*, 134, 105299. <https://doi.org/10.1016/j.envint.2019.105299>
30. Sissakian, V., et al. (2013). Sand and dust storm events in Iraq. *Natural Science*, 5(10), 1084–1094.

31. Stafoggia, M., et al. (2013). Susceptibility factors to ozone-related mortality. *American Journal of Respiratory and Critical Care Medicine*, 188(8), 996–1004.
32. Veefkind, J. P., Aben, I., McMullan, K., et al. (2012). TROPOMI on the ESA Sentinel-5 Precursor: First year in orbit. *Remote Sensing of Environment*, 120, 70–
83. <https://doi.org/10.1016/j.rse.2011.09.027> <https://cds.climate.copernicus.eu/cdsapp#!/dataset/satellite-sentinel-5p-no2>
33. World Health Organization. (2021). WHO global air quality guidelines: Particulate matter.
34. World Meteorological Organization. (2021). Sand and dust storm warning advisory and assessment system annual report 2021.
35. Zuur, A. F., et al. (2009). *Mixed effects models and extensions in ecology with R*. Springer.